sites I and I' becomes important. The QC method should be prefered whenever possible, but the BW formalism is important because of its very transparent formulas, which make it possible to write down the equations as soon as the structure is known.

The parameters have physical significance: the site energy level differences were found to increase in the order $Na^+ > Sr^{2+} > Ca^{2+}$. The site preferences for monovalent cations are I > II > I' and for divalent cations I > I' ≥ II.

Acknowledgment. The authors are indebted to the Belgisch National fonds voor Wetenschappelijk Onderzoek (N.F.W.O.) for research positions as Research Assistant (J.J.V.D.) and Research Director (W.J.M.). The authors thank the Fonds voor Kollektief en Fundamental Onderzoek (F.K.F.O.) for financial assistance.

Supplementary Material Available: Listings of positional parameters, population parameters, temperature factors, agreement factors, and bond distances and angles (2 pages). Ordering information is given on any current masthead page.

Molecular Dynamics Study of an Aqueous $SrCl_2$ Solution

E. Spohr, G. Pálinkás,† K. Heinzinger,*

Max-Planck-Institut für Chemie (Otto-Hahn-Institut), D-6500 Mainz, Federal Republic of Germany

P. Bopp,

Institut für Physikalische Chemie, Technische Hochschule Darmstadt, D-6100 Darmstadt, Federal Republic of Germany

and M. M. Probst

Institut für Anorganische und Analytische Chemie, Universität Innsbruck, A-6020 Innsbruck, Austria
(Received: April 25, 1988)

A molecular dynamics simulation of a 1.1 *m* $SrCl_2$ solution was performed with an improved central force model for water at the experimental density at room temperature. The ion–water and ion–ion potentials were derived from ab initio calculations. The simulation extended over 4 ps at an average temperature of 298 K. The structural properties of the solution are discussed on the basis of radial distribution functions and the orientation of the water molecules and their geometrical arrangement in the hydration shells of the ions. The dynamical properties are calculated from various autocorrelation functions. Results are presented for the influence of the ions on self-diffusion coefficients, hindered translations, librations, and internal vibrations of the water molecules.

1. Introduction

The structures of 1.1 *m* aqueous $BeCl_2$,[1] $MgCl_2$,[2,3] and $CaCl_2$[4,5] solutions have been reported in a series of papers in recent years. The results have been derived from combined molecular dynamics (MD) simulations and X-ray diffraction studies. It has been found that the hydration numbers and the hydration shell structures of the alkaline-earth ions change with increasing ion size in a way which is quite different from that of the singly charged ions.[6] The six water molecules in the first hydration shell of Li^+ prefer an octahedral arrangement with some distortions about the octahedral positions. With increasing alkali-metal ion size the distributions around the octahedral positions broaden, resulting in a uniform distribution of the eight water molecules in the first hydration shells of K^+ and Cs^+. The six water molecules around Mg^{2+} form again a well-defined octahedron, but the 9 or 10 water molecules in the first hydration shell of Ca^{2+}—also well ordered—do not show any regular symmetry.[5] The hydration numbers of all singly charged ions increase linearly with the ion–oxygen first-neighbor distance. The strong change from 6 to 9.2 which occurs in going from Mg^{2+} to Ca^{2+} seems to follow a different trend.[6]

The recent investigation of a $BeCl_2$ solution did not contribute to the clarification of this difference between the alkali-metal and alkaline-earth ions. The X-ray measurements of a 5.3 *m* solution indicate a hydration number for Be^{2+} of 4 in agreement with several NMR measurements, but at a concentration of 1.1 *m* they do not allow a definite conclusion because of the low scattering power of Be^{2+} for X-rays. The MD simulation of the 1.1 *m* solution leads to six octahedrally arranged water molecules in the first shell of Be^{2+}. However, there also remains some doubt on the reliability of these results because pair potentials have been employed in the simulation which might not be sufficient for a correct description of the strong interactions between a water molecule and the small Be^{2+}.[1]

While work is in progress concerning the development of a three-body potential for the Be^{2+}–H_2O interactions, it seemed to be of interest to continue these investigations by the simulation of a 1.1 *m* aqueous $SrCl_2$ solution. In the section 2 the ab initio calculations on which the various pair potentials are based are described and some details of the simulation are given. The structural properties of the solution are discussed in section 3 on the basis of radial distribution functions and the orientation of the water molecules in the first hydration shells of the ions and their geometrical arrangement. Also in section 3 the dynamical properties of the solution such as self-diffusion coefficients and the spectral densities of hindered translations, librations, and

† Permanent address: Central Research Institute for Chemistry of the Hungarian Academy of Sciences, H-1025 Budapest, Hungary.

(1) Yamaguchi, T.; Ohtaki, H.; Spohr, E.; Pálinkás, G.; Heinzinger, K.; Probst, M. M. *Z. Naturforsch., A: Phys., Phys. Chem., Kosmophys.* **1986**, *41*, 1175.
(2) Dietz, W.; Riede, W. O.; Heinzinger, K. *Z. Naturforsch, A: Phys., Phys. Chem., Kosmophys.* **1982**, *37*, 1038.
(3) Pálinkás, G.; Radnai, T.; Dietz, W.; Szász, Gy. I.; Heinzinger, K. *Z. Naturforsch., A: Phys., Phys. Chem., Kosmophys.* **1982**, *37*, 1049.
(4) Probst, M. M.; Radnai, T.; Heinzinger, K.; Bopp, P.; Rode, B. M. *J. Phys. Chem.* **1985**, *89*, 753.
(5) Pálinkás, G.; Heinzinger, K. *Chem. Phys. Lett.* **1986**, *126*, 251.
(6) Heinzinger, K.; Pálinkás, G. In *Interactions of Water in Ionic and Nonionic Hydrates*; Kleeberg, H., Ed.; Springer Verlag: Berlin, Heidelberg, New York, 1987; pp 1-22.

0022-3654/88/2092-6754$01.50/0

TABLE I: Optimized Sr^{2+}–O Distances and Sr^{2+}–H_2O Binding Energies for Different Basis Sets

set	r_{SrO}, Å	$-E$, kJ/mol	t^a	ref
MIDI**[b]	2.527	188.0	38	12
MINI	2.530	175.4	10	12
HW10	2.505	215.6	3	13
HW2	2.518	213.5	2	13
HW2**	2.504	189.7	5	13

[a] Relative time needed for one SCF calculation. [b] The double asterisk indicates that p-type polarization functions for Sr^{2+} [12] and H[14] and d-type ones for O[14] were used to augment the basis sets.

internal vibrations are derived from the simulations with the help of various autocorrelation functions.

2. Interaction Potentials and Details of the Simulation

All intermolecular potentials in the simulation presented here were of the pair potential type and consisted of a Coulomb part for which the Ewald summation was applied and of short-range parts for which the shifted force method was used.[7]

Water is described by a model which treats the intermolecular O–O, O–H, and H–H interactions by means of the latest version of the central force (CF) model[8] (with the exception of a minor technical modification[23]) but uses a three-body potential for a more correct description of the intramolecular interactions.[9,10] This modification has led to a marked improvement with respect to the intramolecular vibrational motions and the dissociation energy of the water molecules.[10,11] As the intermolecular part of the potential is very similar to the one employed in previous work, no model dependence is expected for the data obtained with this improved model, and a direct comparison is thus possible with the results of simulations of $BeCl_2$, $MgCl_2$, and $CaCl_2$ solutions.

For the Sr^{2+}–O, Sr^{2+}–H, Sr^{2+}–Sr^{2+}, and Sr^{2+}–Cl^- interactions new Hartree–Fock calculations have been performed since ab initio calculations on the strontium–water system could not be found in the literature. Sr^{2+} with its 36 electrons is a rather large ion from the viewpoint of quantum mechanical calculations, and not many ab initio calculations have been reported. Therefore, a number of test calculations were performed in order to find a basis that allows a sufficiently accurate evaluation of the potential hypersurface with a still reasonable amount of computer time. In particular, the results of standard Hartree–Fock calculations have been compared with effective core potential (ECP) SCF calculations in which some of the inner electronic shells are decoupled from the valence electrons, resulting in faster calculations and reduced superposition errors. Regarding computer time, it was also important to answer the question whether the eight N-shell electrons can be attributed to the core or if they must be treated as Hartree–Fock valence electrons.

The optimized Sr^{2+}–O distances and Sr^{2+}–H_2O binding energies are given in Table I for different basis sets. MIDI and MINI denote Huzinaga's all-electron basis sets in double-ζ and single-ζ contraction, respectively.[12] HW10 and HW2 are ECP basis sets from Hay and Wadt.[13] In HW2 the N shell of strontium is attributed to the core while in HW10 it is left in the valence space. The DZP basis set of Dunning[14] was used for the water molecule when the all-electron basis sets were employed for Sr^{2+}. In all other calculations Dunning's oxygen basis set was replaced by an ECP one from Stevens et al.[15]

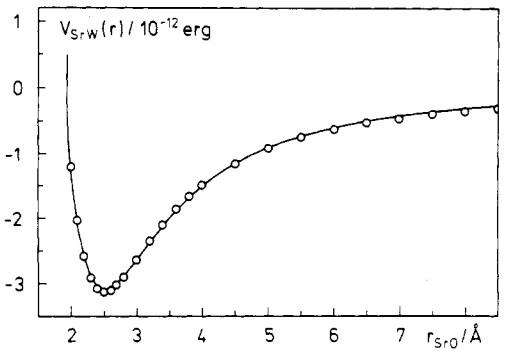

Figure 1. Fitted strontium–water potential for C_{2v} geometry. Circles indicate energy values from ab initio calculations.

TABLE II: Pair Potentials Employed in the Simulation[a]

$V_{OO}(r) = 10.04/r + 1858/r^{8.86} - 0.01736\{\exp[-4(r - 3.4)^2] + \exp[-1.5(r - 4.5)^2]\}$
$V_{OH}(r) = -5.019/r + 0.433/r^{9.2} - 0.694/\{1 + \exp[40(r - 1.05)]\} - 0.278/\{1 + \exp[5.493(r - 2.2)]\}$
$V_{HH}(r) = 2.509/r + 6.957/\{1 + \exp[29.9(r - 1.968)]\}$
$V_{SrO}(r) = -30.43/r - 19.79/r^2 + 2929 \exp(-3.11r)$
$V_{SrH}(r) = 15.22/r + 5.85/r^2 + 0.24 \exp(-0.158r)$
$V_{SrSr}(r) = 92.27/r - 0.999/r^2 + 0.4437 \exp(-0.617r)$
$V_{SrCl}(r) = -46.14/r - 22.75/r^2 + 1344 \exp(-2.14r)$
$V_{ClO}(r) = 15.22/r - 1.849/r^2 + 6304 \exp(-3.21r)$
$V_{ClH}(r) = -7.609/r + 3.138 \times 10^{24} \exp(-34r)$
$V_{ClCl}(r) = 23.07/r - 476.1r^6 + 15230 \exp(-3.39r)$

[a] Energies are given in 10^{-12} erg and distances are in Å. For intramolecular potentials see ref 9.

If it is assumed that the calculations with the MIDI** basis set lead to the most accurate results, then all other distances and energies presented in Table I are within the limits of uncertainty expected at the Hartree–Fock level. The results achieved with the MINI basis set, which has only single-ζ quality, do not deviate too much from the ones with MIDI**, thus indicating a rather small basis set superposition error for this system. It is even more important to note that only a small difference exists between HW2 and HW10. A breakdown of the ECP approximation would have led to much too short Sr^{2+}–O distances in the HW2 case.

Finally, it was decided to use the HW2** basis set for the calculation of the whole potential surface as the polarization functions might somewhat improve the accuracy of the energy points for orientations outside the C_{2v} symmetry. Altogether about 250 points were calculated by moving the Sr^{2+} around a water molecule. The energy curve for the C_{2v} symmetry contains the global minimum and is shown in Figure 1. Similar calculations were performed for the one-dimensional Sr^{2+}–Sr^{2+} and Sr^{2+}–Cl^- pair potentials. For both ions MIDI** basis sets were used. In the case of Sr^{2+}–Sr^{2+} no significant deviation from a purely electrostatic potential could be seen.

As in previous work,[1,2,4] a single analytical function with three adjustable parameters was fitted to the energy points after the Coulombic contributions—determined by the water model and the ionic charges—had been subtracted from the interaction energies. The Cl^-–O, Cl^-–H, and Cl^-–Cl^- interactions were taken from the $MgCl_2$ simulation.[2] They have been derived in the same way as described for Sr^{2+}. The final pair potentials are listed in Table II.

The basic cube contained 200 water molecules, 4 cations, and 8 anions representing a 1.1 m $SrCl_2$ solution. The side length of the cube of 18.32 Å corresponds to the experimental density at room temperature of 1.145 g/cm^3. A suitably scaled configuration from the simulation of a 1.1 m $MgCl_2$ solution served as starting configuration. After several thousand time steps of equilibration the collection of data was started; the simulation was performed for about 16 000 time steps of 2.5×10^{-16}s each, leading to a total elapsed time of about 4 ps. The average temperature of the system

(7) Streett, W. B.; Tildesley, D. J.; Saville, G. *ACS Symp. Ser.* **1978**, *86*, 144.
(8) Stillinger, F. H.; Rahman, A. *J. Chem. Phys.* **1978**, *68*, 666.
(9) Bopp, P.; Jancsó, G.; Heinzinger, K. *Chem. Phys. Lett.* **1983**, *98*, 129.
(10) Jancsó, G.; Bopp, P. *Z. Naturforsch., A: Phys., Phys. Chem., Kosmophys.* **1983**, *38*, 206.
(11) Probst, M. M.; Bopp, P.; Heinzinger, K.; Rode, B. M. *Chem. Phys. Lett.* **1984**, *106*, 317.
(12) Huzinaga, S., Ed. *Physical Sciences Data*; Elsevier: Amsterdam, 1984; Vol. 16.
(13) Hay, P.; Wadt, W. R. *J. Chem. Phys.* **1985**, *82*, 284, 299.
(14) Dunning, T. H. *J. Chem. Phys.* **1970**, *53*, 2823.
(15) Stevens, W. J.; Basch, H.; Krauss, M. *J. Chem. Phys.* **1984**, *81*, 6026.

TABLE III: Characteristic Values for the Radial Distribution Functions $g_{\alpha\beta}(r)$[a]

α	β	R_1	r_{M_1}	$g_{\alpha\beta}(r_{M_1})$	R_2	r_{m_1}	$g_{\alpha\beta}(r_{m_1})$	$n_{\alpha\beta}(r_{m_1})$	r_{M_2}	$g_{\alpha\beta}(r_{M_2})$
Sr	O	2.44	2.63	10.6	2.99	3.18	0.10	9.8	≈5.0	1.95
Sr	H	3.04	3.35	4.90	3.68	4.00	0.13	20.1	5.35	1.69
Cl	O	2.94	3.18	3.49	3.57	3.95	0.64	7.8	–	–
Cl	H	1.98	2.22	2.98	2.58	2.86	0.46	6.5	3.48	1.44
O	O	2.64	2.85	3.00	3.19	≈3.4	0.80	5.1	4.85	1.18
O	H	1.72	1.93	1.23	2.17	2.45	0.21	3.8	3.23	1.54
H	H	2.17	2.30	1.55	2.73	3.05	0.78	6.7	3.74	1.15

[a] R_i, r_{M_i}, and r_{m_i} are the distances in Å where for the ith time $g_{\alpha\beta}(r)$ is unity, a maximum, and a minimum, respectively. For O–H and H–H only intermolecular data are given.

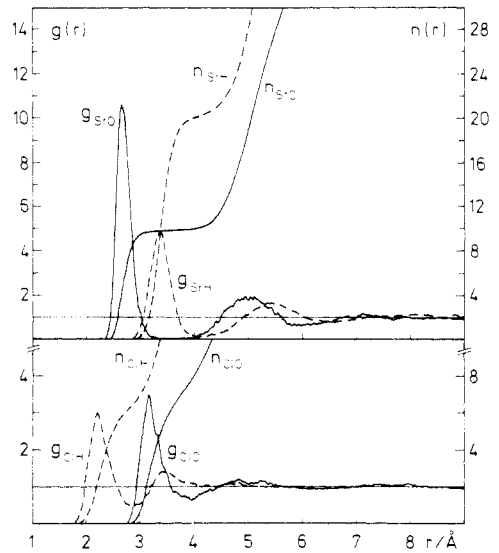

Figure 2. Ion–oxygen and ion–hydrogen radial distribution functions and running integration numbers.

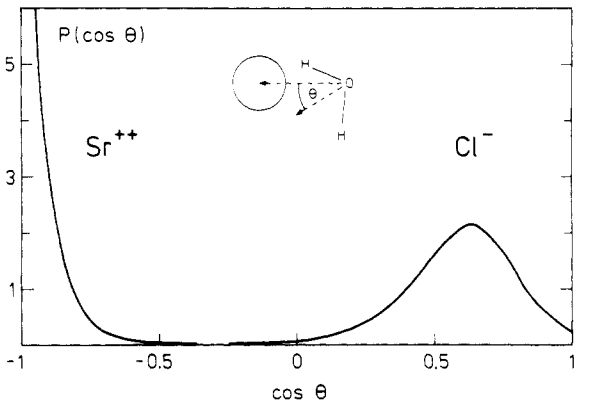

Figure 3. Distributions of cos θ for the water molecules in the first hydration shells of Sr^{2+} and Cl^-. θ is defined in the insert.

was 298 K, and no rescaling of the velocities was performed during the run in order to be able to obtain reliable velocity autocorrelation functions.[16] The total energy was stable to better than 0.1% during the whole run.

3. Results and Discussion

(*a*) *Radial Pair Distribution Functions (RDF).* Figure 2 shows the RDFs $g_{\alpha\beta}(r)$ for ion–oxygen and ion–hydrogen and the corresponding running integration numbers $n_{\alpha\beta}(r)$, defined by

$$n_{\alpha\beta}(r) = 4\pi\rho_0 \int_0^r g_{\alpha\beta}(r')r'^2\,dr' \qquad (1)$$

where ρ_0 is the number density of the atoms of kind β. In Table III some of the characteristic values for the various RDFs are listed.

The first peak in the Sr^{2+}–O RDF is centered at 2.63 Å, which is by about 0.1 Å larger than the distance at which the minimum of the Sr^{2+}–water pair potential for the C_{2v} geometry has been found. About the same difference between the position of the first ion–oxygen peak and the minimum of the pair potential has been observed for the other alkaline-earth ions investigated so far, while in the case of the alkali-metal and halide ions both distances almost coincide. The stronger ion–water interactions in the case of doubly charged ions lead to repulsive forces between the water molecules in the first hydration shells and thus may prevent an approach of the water molecules to the distances of the potential minima. The lower height of the first peak $g_{SrO}(r)$ compared with the ones for Be^{2+}, Mg^{2+}, and Ca^{2+} is in keeping with the larger size of Sr^{2+}. As in the case of the other alkaline-earth ions, a pronounced second peak in $g_{SrO}(r)$ exists which is well separated from the first peak. A hydration number of 9.8 is found for Sr^{2+} which is only by 0.6 larger than the one for Ca^{2+} while the increase from Mg^{2+} to Ca^{2+} was 3.2.

X-ray measurements by Albright[17] and by Caminiti et al.[18] on $SrCl_2$ solutions have led to Sr^{2+}–O first-neighbor distances of 2.6 and 2.64 Å, respectively, in agreement with the results from the simulation. The hydration number of 7.9 for Sr^{2+} deduced from the experiment by Albright is significantly lower than the one found here. This discrepancy might result from the difficulty of determining a reliable hydration number from X-ray experiments. The value of 8 reported by Caminiti et al. was determined by a model fit.

The positions and heights of the first and second peak in the Sr^{2+}–H RDF change relative to the other alkaline-earth ions as expected from the size of Sr^{2+}. The running integration number of $g_{SrH}(r)$ at the first minimum gives about 20 in agreement with the hydration number of 9.8.

The positions of the peaks in the Cl^-–O and Cl^-–H RDFs are the same, in the limits of statistical uncertainty, for all alkaline-earth chloride solutions investigated. The heights of the first peaks in both RDFs increase with increasing counterion size, which in turn leads to a slight increase in the hydration number of Cl^-. This means that already in the 1.1 *m* solutions the structure of the hydration shell of the anions is influenced by the size of the doubly charged cations.

The O–O, O–H, and H–H RDFs in the 1.1 *m* $SrCl_2$ solutions are in the limits of statistical uncertainty the same as for the $CaCl_2$ solution.[4] Therefore, they are not shown here.

(*b*) *Orientation of the Water Molecules.* The distributions of cos θ for the water molecules in the first hydration shells of Sr^{2+} and Cl^- are shown in Figure 3. θ is defined as the angle between the dipole moment direction of the water molecule and the vector pointing from the oxygen atom toward the center of the ion. Figure 3 shows for Sr^{2+} a strong preference for a trigonal orientation. The distribution is slightly broader than that for Ca^{2+}.[4] The water molecules in the first hydration shell of Cl^- form preferentially linear hydrogen bonds, with a distribution which is very similar to the one found for the 1.1 *m* $CaCl_2$ solution.

(*c*) *Hydration Shell Structures.* From the knowledge of the position of all particles as a function of time provided by the MD simulation, the geometrical arrangement of the water molecules

(16) Hermansson, K.; Lie, G. C.; Clementi, E. *J. Comput. Chem.* **1988**, *9*, 200.

(17) Albright, J. N. *J. Chem. Phys.* **1972**, *56*, 3783.

(18) Caminiti, R.; Musinu, A.; Paschina, G.; Pinna, G. *J. Appl. Crystallogr.* **1982**, *15*, 482.

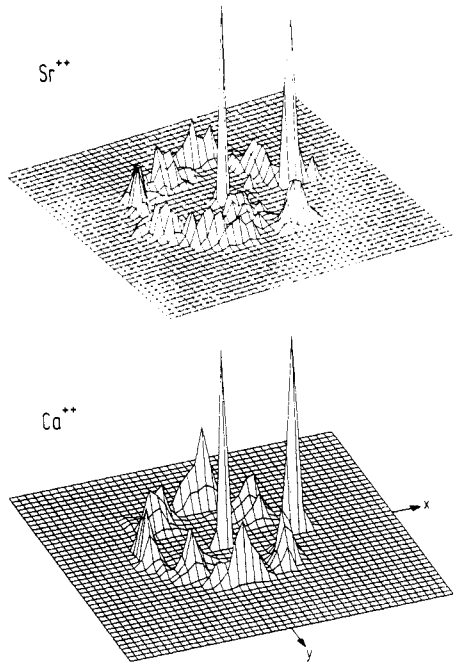

Figure 4. Densities of the projections of the oxygen atom positions of the 10 nearest-neighbor water molecules around Sr^{2+} and Ca^{2+} onto the xy plane of a coordinate system as defined in the text.

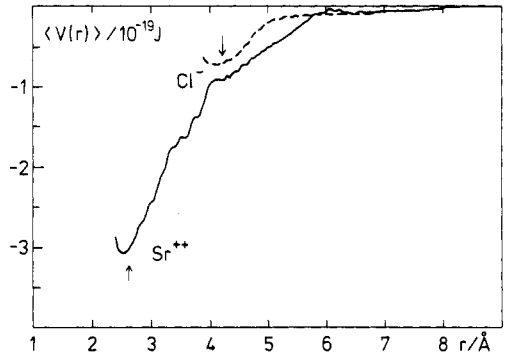

Figure 5. Average potential energy of a water molecule with respect to Sr^{2+} and Cl^- as a function of the ion–oxygen distance. The positions of the first maxima in the RDFs are marked by arrows.

in the first hydration shells of the ions has been deduced. In order to achieve this a coordinate system has been introduced where the ion defines the origin, one oxygen atom of the hydration shell water molecules the z axis, and a second one the xz plane. plane. The densities of the projections of the oxygen atom positions of the 10 nearest-neighbor water molecules around Sr^{2+}—collected at several hundred time steps spread over the whole simulation—onto the xy plane of this coordinate system are shown in Figure 4 in the form of an axonometric drawing and compared with that for Ca^{2+}. The distribution of the eight water molecules in the first hydration shell of Cl^- is found to be uniform just as in all other chloride solutions investigated so far and is, therefore, not shown here.[6]

Figure 4 shows clearly that with increasing ion size (the ion–oxygen first-neighbor distances are 2.39 and 2.63 for Ca^{2+} and Sr^{2+}, respectively) there is a tendency for a more uniform distribution of the water molecules in the first hydration shells. This result is not unexpected but quite different from the strong change from an octahedral symmetry found for Mg^{2+} to the well-ordered hydration shell of Ca^{2+} which has no regular symmetry.[6]

(*d*) *Average Potential Energy.* Figure 5 shows the average potential energy of a water molecule with respect to Sr^{2+} and Cl^- as a function of the ion–oxygen distance. The positions and depths of the minima in the $\langle V(r) \rangle$ curves are very similar to those of the pair potentials. This indicates that no strong hindrance prevents the water molecules from orienting themselves favorably with respect to the ion. The maxima of the ion–oxygen RDFs,

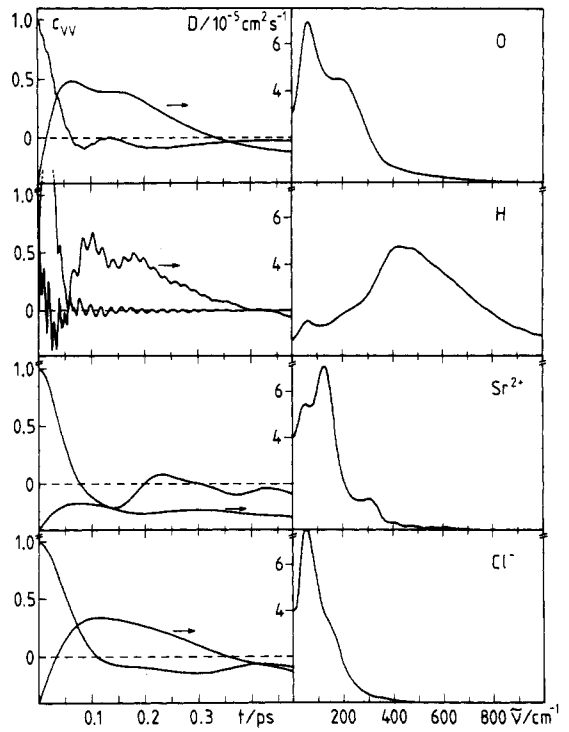

Figure 6. Normalized velocity autocorrelation functions for oxygen atoms, hydrogen atoms, Sr^{2+}, and Cl^-, their running integrations according to eq 2, and spectral densities in arbitrary units in the frequency range $0 < \tilde{\nu} < 1000$ cm^{-1}.

which are marked in Figure 5 by arrows, appear at a slightly larger distance than the minima in $\langle V(r) \rangle$. This difference shows that there is not enough space available in the hydration shells for all water molecules to settle at the distance of the potential energy minimum (see above).

(*e*) *Self-Diffusion Coefficients.* Figure 6 shows the normalized velocity autocorrelation functions $C_{vv}(t)/C_{vv}(0)$ for the oxygen atoms, the hydrogen atoms, and for Sr^{2+} and Cl^-. Also given are the integrals

$$D_i(t) = \tfrac{1}{3} \int_0^t C^i_{vv}(t')\, dt' \qquad (2)$$

which in the limit $t \to \infty$ converge toward the self-diffusion coefficients of species i. The autocorrelation function (acf) of a quantity a_i—with a_i either a scalar or a vector—is calculated from the simulation by

$$C^i_{aa}(t) = \frac{1}{N_T N} \sum_{i=1}^{N} \sum_{j=1}^{N_T} a_i(t_j)\, a_i(t_j+t) \qquad (3)$$

where N denotes the number of particles and N_T the number of time averages. The various acfs are shown in Figure 6 only up to a lengths of 4.75×10^{-13} s in all four cases to ease the comparison, in spite of the fact that the motional regimes are obviously very different. It is also clear that this length is not sufficient to converge eq 2 to the self-diffusion coefficients.

The self-diffusion coefficient of Cl^- is found to be $(1.2 \pm 0.3) \times 10^{-5}$ cm^2 s^{-1}. In the limits of the relatively large statistical uncertainty this value is the same as found from simulations of 2.2 m NaCl,[19] KCl,[20] and NH_4Cl[21] solutions. The result indicates that at moderate concentrations D_{Cl^-} does not depend strongly on the cation. The value for Sr^{2+} of $(0.6 \pm 0.1) \times 10^{-5}$ cm^2 s^{-1} is lower than that for Na^+, K^+, and NH_4^+ but is the same in the

(19) Jancsó, G.; Heinzinger, K.; Bopp, P. *Z. Naturforsch., A: Phys., Phys. Chem., Kosmophys.* **1985**, *40*, 1235.
(20) Migliore, M.; Fornili, S. L.; Spohr, E.; Heinzinger, K. *Z. Naturforsch., A:* Phys., *Phys. Chem., Kosmophys.* **1987**, *42*, 227.
(21) Szász, Gy. I.; Riede, W. O.; Heinzinger, K. *Z. Naturforsch., A: Phys., Phys. Chem., Kosmophys.* **1979**, *34*, 1083.

limits of error as for Li^+ when calculated from a simulation of a 2.2 *m* LiI solution.[22] The self-diffusion coefficients of the cations in electrolyte solutions depend not only upon their masses but also on their charges and sizes as the latter two properties are responsible for the strength of the interactions between the ion and its hydration shell water molecules. In order to investigate this complicated interdependence by MD simulations, a much higher accuracy would be needed than the one possible for the time being.

An important advantage of the MD simulations is the possibility of calculating the single ion effects on the motions of the water molecules. This is achieved by subdividing the 200 water molecules into three subsystems: hydration water of the cation (cw), hydration water of the anion (aw), and bulk water (bw). The first hydration shells are defined in terms of cation–oxygen and anion–hydrogen distance (here $r(Sr^{2+}–O) \leq 3.8$ Å and $r(Cl^-–H) \leq 2.75$ Å), leading to an average of 39.7 molecules contributing to the cw functions and 48.7 molecules contributing to the aw functions. The subdivision into the three classes is only carried out at correlation origin (t_j in eq 3). The exchange of water molecules between the three classes is assumed to be negligible during the typical lengths of the correlations.

The self-diffusion coefficients for bulk water and hydration water of Cl^- are the same in the limits of statistical uncertainty $(1.4 \pm 0.2) \times 10^{-5}$ cm^2s^{-1}, while the one for the hydration water of Sr^{2+} is smaller by about 35% than that of bulk water. The difference in the self-diffusion coefficients between the hydration water of anion and cation results from the difference in strength of the ion–water interactions (see, e.g., Figure 2). Even stronger reductions than for Sr^{2+} have been reported earlier for the hydration water of the Li^+.[22] For the hydration water of Cl^-, both slight reductions (in NaCl[19] and KCl[20] solutions) and slight increases (in NH_4Cl solutions[21]) of the self-diffusion coefficients have been reported, indicating a slight counterion dependence. The self-diffusion coefficients for both ions are significantly smaller than the ones of their hydration water.

Although it is well-known that the central force model leads to too low absolute values for the self-diffusion coefficient, the present model has been shown to reproduce the pressure dependence of the self-diffusion coefficient in pure water reasonably well.[23] Therefore, the results presented here seem to be reliable at least in their relation to each other.

(f) Hindered Translations. The Fourier transforms of the velocity autocorrelation functions for the various atoms in the aqueous $SrCl_2$ solution—as shown in the left side of Figure 6—are presented in the right column for frequencies up to 1000 cm^{-1}. The Fourier transforms for Sr^{2+}, Cl^-, and O represent the spectral densities of the hindered translational motions for the ions and all water molecules in the solution, where in the O case the librations of the water molecules also contribute slightly. In the case of the H atoms it mainly reflects the librational motions of the water molecules and will be discussed in more detail in the next section. As in the case of the self-diffusion coefficients, the hindered translations, librations, and internal vibrations of the water molecules have been calculated separately for the three water subsystems as defined above in order to reach a better understanding of the single ion effect on the motions of the water molecules.

The Cl^- spectrum consists of a main peak at 50 cm^{-1} with a shoulder on the high-frequency side at about 120 cm^{-1} extending to roughly 200 cm^{-1}. It is similar to the spectrum observed for this ion in a NaCl solution[19] with the same water model and in a KCl solution[20] with the ST2 model. A simulation of an NH_4Cl solution[21] with the ST2 water has led to a somewhat lower intensity on the high-frequency side. The 50-cm^{-1} peak has been assigned to the hindered translational motions of the bare Cl^-, while the high-frequency shoulder is expected to result from the interactions of the Cl^- with its hydration shell water molecules.[24]

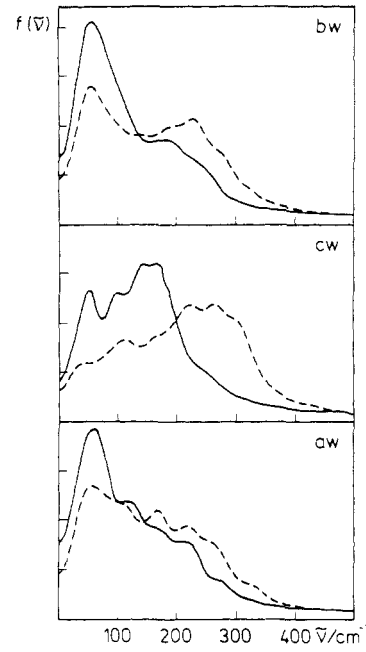

Figure 7. Spectral densities of the hindered center-of-mass motions perpendicular (solid) and parallel (dashed) to the plane of the water molecules, calculated separately for the three subsystems bulk water (bw), hydration water of the cation (cw), and hydration water of the anion (aw) and given in arbitrary units.

The Sr^{2+} spectrum shows a main peak at 125 cm^{-1} and two smaller ones at 50 and 300 cm^{-1}. The main peak and the one at 50 cm^{-1} seem to correspond to the peaks found for the hindered translational motions of the hydration shell water molecules perpendicular to the molecular plane, while the high-frequency peak corresponds to the peak found for the motions parallel to the plane (Figure 7). The latter one may thus be identified with mostly stretching-type motions between ion and hydrated water molecules, while the former ones should correspond to more out-of-plane wagging motions. This point will further be discussed below. A similar coupling of the hindered translational motion of an ion with the librations of its hydration shell molecules has been found for Li^+ in the frequency range 600–800 cm^{-1}.[25]

The spectral densities of the hindered translational motions of all water molecules in the $SrCl_2$ solution as calculated from the velocity acf of the O atoms (Figure 6) are very similar to those of pure water[23] and show a maximum at 50 cm^{-1} and a pronounced shoulder at 200 cm^{-1} which have been attributed to the hydrogen bond bending and the O–O stretching motions, respectively.[26] In Figure 7 the spectral densities are presented separately for the three water subsystems and for the motions perpendicular (solid) and parallel (dashed) to the plane of the water molecule, calculated from the center-of-mass velocities. Figure 7 shows that in all three subsystems the motions parallel to the plane of the molecule contribute more to the high-frequency region than the ones perpendicular to the plane. Keeping in mind the three-dimensional structure of water, it appears—in accordance with the assignment of the two frequencies—that almost any motion parallel to the molecular plane involves the stretch of a hydrogen bond while motions perpendicular to the plane of the molecule involve mostly the bending of bonds.

The spectral densities for the hydration water of Cl^- are similar to the ones for bulk water, except that the motions of the molecules seem to be more isotropic here. There are no significant differences between these spectra and the ones for pure water.[23] The same conclusion has been drawn from other simulations of electrolyte solutions with Cl^- as anion.[19,21,22] The hydration water of the Cl^- is thus dynamically still quite similar to bulk water which is in keeping with the structure of the hydration shell discussed above.

(22) Szász, Gy. I.; Heinzinger, K.; Riede, W. O. *Ber. Bunsen-Ges. Phys. Chem.* **1981**, *85*, 1056.
(23) Jancsó, G.; Bopp, P.; Heinzinger, K. *Chem. Phys.* **1984**, *85*, 377.
(24) Heinzinger, K. *Physica B+C (Amsterdam)* **1985**, *131B*, 196.
(25) Szász, Gy. I.; Heinzinger, K. *J. Chem. Phys.* **1983**, *79*, 3467.
(26) Sceats, M. G.; Rice, S. A. *J. Chem. Phys.* **1980**, *72*, 3236.

TABLE IV: Frequencies, in cm^{-1}, of the Peak Maxima of the Spectral Densities of the Librations and Vibrations for All Water Molecules in the Solution and Separately for the Three Water Subsystems As Defined in the Text[a]

		total water	bulk water	hydration water	
				cation	anion
R_x	$\tilde{\nu}_{max}$	445 ± 10	410 ± 10	500 ± 10	465 ± 10
R_y	$\tilde{\nu}_{max}$	620 ± 10	595 ± 10	640 ± 15	650 ± 15
R_z	$\tilde{\nu}_{max}$	405 ± 10	405 ± 10	390 ± 10	420 ± 20
Q_1	$\tilde{\nu}_{max}$	3450 ± 10	3475 ± 10	3335 ± 10	3420 ± 10
	$\Delta\tilde{\nu}$		230 ± 10	230 ± 10	360 ± 10
Q_2	$\tilde{\nu}_{max}$	1705 ± 5	1705 ± 5	1690 ± 10	1710 ± 10
	$\Delta\tilde{\nu}$		165 ± 10	150 ± 10	180 ± 10
Q_3	$\tilde{\nu}_{max}$	3580 ± 10	3595 ± 10	3460 ± 10	3540 ± 20
	$\Delta\tilde{\nu}$		260 ± 10	270 ± 10	330 ± 10

[a] In the case of the vibrations the widths at half-height, $\Delta\tilde{\nu}$, are given additionally.

The spectral densities of the perpendicular and parallel motions of the hydration water molecules of the Sr^{2+} are completely different from the ones for bulk water. They are strongly anisotropic. The spectral density of the parallel motions has a maximum at about 250 cm^{-1} while the one for the perpendicular motions shows two maxima. The peak at about 50 cm^{-1} can be considered a remnant of the bulk water one and appears on top of a broad and somewhat asymmetric band with a maximum at about 180 cm^{-1} and extending to about 350 cm^{-1}. The dynamical behavior of these molecules is clearly dominated by forces different from the ones prevailing in the bulk. With the structure of the hydration shell in mind one may conclude that the motions parallel to the plane are mostly controlled by the strong ion–water interactions while the ones perpendicular to the plane result from repulsions between neighboring water molecules in the hydration shell. The small peak visible at the position of the O–O–O bending peak in pure water may be taken as an indication of to what extent the hydrated water molecules participate in hydrogen bonds with their neighbors in the bulk. Experimental values for the ion–water vibrational frequencies are not available for the Sr^{2+} ion. For comparison, values of 359 and 290 cm^{-1} have been reported for this vibration of water molecules hydrated to Mg^{2+} and Ca^{2+}, respectively.[27] It is reasonable to expect that the corresponding value for Sr^{2+} should be lower.

(*g*) *Librational Motions.* In order to calculate the various librational and vibrational modes from the velocity acfs of the hydrogen atoms, a scheme has been developed which is described in the Appendix. The application of this scheme leads to the spectral densities of the librations around the three main axes of the water molecules. The results are presented separately for the three water subsystems in Figure 8. The positions of the maxima of the librational spectra are given in Table IV.

The librational spectra for bulk water are quite similar to the ones for pure water. The maxima of the spectral densities for the librations around the x and z axes appear at about 400 cm^{-1} while the smaller moment of inertia for the rotation around the y axis leads to a broad peak centered at about 600 cm^{-1}. The positions of the maxima resulting from the simulation with ST2 water differ from the ones presented here only as far as the high-frequency libration is concerned (≈800 cm^{-1}). It seems to be mainly a consequence of the differences in water molecule geometry between the two models (larger HOH angle for ST2 water).

Both ions cause a significant blue shift of the librational frequencies around the x and y axes relative to bulk water while the maxima in the spectral densities for the rotations around the dipole moment axis show only small changes, hardly outside the limits of statistical uncertainty (Figure 8 and Table IV). The effect of anion and cation on the peak maximum of the librations around the y axis is quite similar while the shift caused by Sr^{2+} in the case of the x axis is about twice as large as that of Cl^-.

(27) Irish, D. E.; Jarv, T. *Faraday Discuss. Chem. Soc.* **1978**, *64*, 95. Kabbim, H. *J. Raman Spectrosc.* **1987**, *18*, 301.

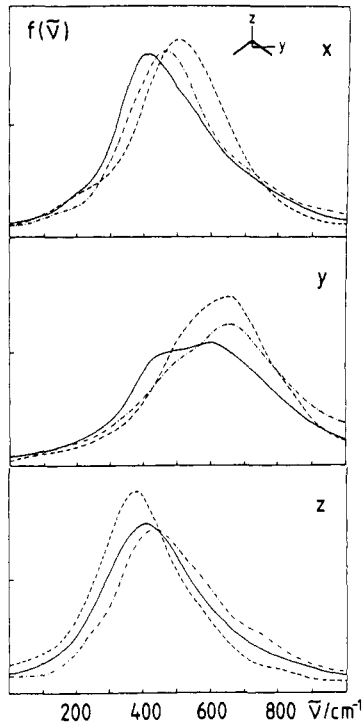

Figure 8. Spectral densities of the librations around the three main axes of the water molecule as defined in the insert, calculated separately for the hydration water of Sr^{2+} (---), Cl^- (-·-), and bulk water (—) and given in arbitrary units.

The strong Sr^{2+}–water interactions lead to a well-defined first hydration shell where the oxygen atom density goes up to about 10 times the average one (Figure 2) and results in a strong preference for an orientation where the dipole moment of the water molecule points away from the center of the ion (Figure 3). Consequently, these water–water interactions cause an additional hindrance for the rotations around the x and y axes which explains the blue shift for the hydration shell molecules while the rotation around the z axis remains rather unaffected. This explanation is in accordance with the results of simulations of 2.2 *m* KCl, NH_4Cl, and LiI solutions with the ST2 model for water. It has been found that K^+ and NH_4^+ do not significantly influence the librational motions of their hydration shell water molecules because of the weaker ion–water interactions compared with Sr^{2+}.[20,21] In contrast, Li^+ causes a blue shift of about 200 cm^{-1} for the librational motions around all three principal axes of the six water molecules in its first hydration shell.[25] The difference between Li^+ and Sr^{2+} as far as the z axis is concerned results from the orientation of this hydration shell molecule. While in the simulations with the ST2 model for water a lone pair orbital is directed toward the cation, a trigonal orientation is found in the case of the CF model.

The small blue shift found for the librational bands of the hydration shell water molecules of Cl^- relative to bulk water might result from the stronger hydrogen bond formed between Cl^- and water than between water and water, which is evident from the corresponding red shift of the O–H stretching vibration (see below).

The single ion effect on the librational motions of the hydration shell water molecules presented here can hardly be detected experimentally since only the changes in the total water of the solution can be compared with pure water. Recent inelastic neutron scattering experiments[28] on salt solutions in light and heavy water showed only small effects with increasing salt concentration for $SrCl_2$ solutions. This is mostly due to the fact that at moderate concentrations—as long as the hydration shells do not overlap—the

(28) Bellisent-Funel, M.-C.; Dianoux, A. J.; Fontana, M. P.; Maisano, G.; Migliardo, P. In *Water and Aqueous Solutions*; Neilson, G. W., Enderby, J. E., Eds.; Adam Hilger: Bristol, 1985; pp 199–206. Bellisent-Funel, M.-C., private communication.

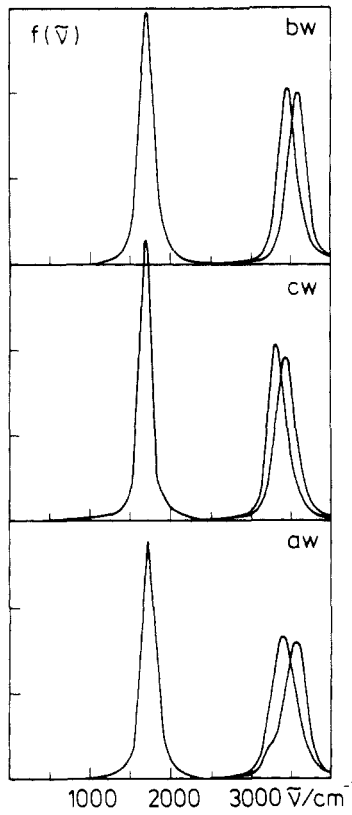

Figure 9. Spectral densities of the three intramolecular vibrational motions of the water molecules in the three water subsystems in arbitrary units.

percentage of bulk water molecules remains so high that only small differences emerge between pure water and the solution. This has also been demonstrated from simulations of the librational motions in a 2.2 *m* LiI solution[25] and the vibrations in a 1.1 *m* $CaCl_2$ solution.[11]

(*h*) *Intramolecular Geometry and Vibrations.* The ion–water interactions lead to an increase of the intramolecular O–H distance and a decrease of the HOH angle for the water molecules in their hydration shells, resulting in average values of 0.9753, 0.9768, and 0.9815 Å as well as 100.7°, 100.3°, and 99.2° for bulk water, hydration water of Cl^-, and hydration water of Sr^{2+}, respectively. These changes in geometry together with the partial charges on the O and H atoms lead to an increase of the dipole moment for the hydration shell water molecules of Sr^{2+} by about 2% compared with bulk water for which a value of 2.00 D has been calculated.

From the well-known empirical relationship between the intramolecular O–H distances and the frequencies of the O–H stretching modes of about 20 000 $cm^{-1}/Å$,[30] red shifts relative to bulk water of about 120 and 30 cm^{-1} are expected for the hydration shell molecules of Sr^{2+} and Cl^-, respectively. The spectral densities of the three normal mode vibrations calculated by Fourier transformation from the acfs of the H-atom velocities—after separation according to the method described in the Appendix—are presented in Figure 9 separately for bulk water and hydration water of Sr^{2+} and Cl^-. The figure shows that symmetric and asymmetric O–H stretching vibrations are well separated, which justifies the approximation described in the Appendix. The frequencies of the peak maxima and the width at half-height have been collected in Table IV.

In the bulk water the positions of all peaks are identical, within the error margins, with the ones found in the bulk water of a $CaCl_2$ solution.[29] The corresponding values for the stretching vibrations in pure water are 3460 ± 15 and 3560 ± 15 cm^{-1} at 300 K and 3475 ± 10 and 3580 ± 10 cm^{-1} at 335 K.[31] With respect to the vibrational frequencies, bulk water thus resembles pure water at a temperature about 30 K higher. The splitting between the two stretching modes is only very slightly increased compared to its gas-phase value of about 105 cm^{-1}, in spite of the gas–liquid frequency shift of about 360 cm^{-1}. The frequency of the bending vibration, shifted to the blue by about 60 cm^{-1} compared to the gas phase, is identical in all cases mentioned above. We also note that, at least with the present model, the peak found for the bending vibrations is markedly narrower than the ones associated with the stretches.

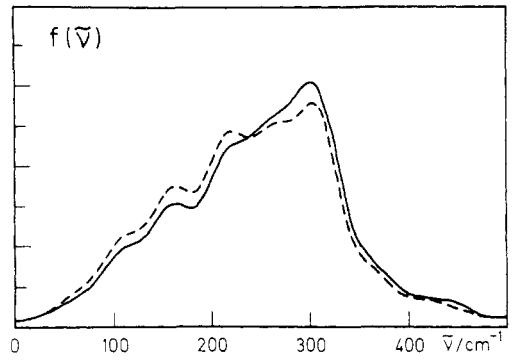

Figure 10. Spectral densities of the symmetric (solid) and asymmetric (dashed) ion–water stretching vibrations of adjacent water molecules in the hydration shell of Sr^{2+}, given in arbitrary units.

The red shift of about 140 cm^{-1} for the O–H stretching vibrations which has been found here for the Sr^{2+} hydration water relative to bulk water is in accordance with the increase of the average O–H distance. It is much smaller than the value of 320 cm^{-1} calculated for Ca^{2+} in a first application of the present flexible water model to the study of intramolecular vibrational frequencies in aqueous solutions.[11] In a preliminary comparative study of several divalent cations, the magnitude of the shifts has been found to depend on the size of the ion as expected.[32] These predictions of a strong cation effect on the O–H stretching frequencies of the hydration shell water molecules from the simulations have recently been confirmed experimentally for several divalent cations.[33] The bending vibration is only slightly affected by the presence of the ions and shifts to the red by about 15 cm^{-1} hardly outside the limits of error. The peaks have approximately the same width as in bulk water.

The weaker interactions between Cl^- and water are reflected in the smaller red shift of the O–H stretching frequencies of about 50 cm^{-1} for the hydration shell molecules relative to bulk water. Again, this shift is in keeping with the increase of the average O–H distance. The bending frequency of the water molecules is not influenced by Cl^-. The width at half-height of all three vibrational peaks is, relative to bulk water, much more strongly increased for the hydration water of Cl^- than for Sr^{2+}. The broader frequency distribution in the case of Cl^- seems to be a consequence of the less pronounced first hydration shell and especially of the broader distribution of cos θ relative to the one for Sr^{2+} (Figure 3).

(*i*) *Collective Motions.* The ion–water stretching vibrations of water molecules in the hydration shell of Sr^{2+} have been studied from their center-of-mass velocities with a procedure similar to the one described in the Appendix for the intramolecular stretches of the water molecules. The ratio of the masses involved is less favorable here for such a simplified procedure than in the water molecule. It is nevertheless expected that qualitative features of the ion–water stretching vibrations can be detected with this method. Figure 10 shows the result. The spectral densities for the symmetric (full) and asymmetric (dashed) stretching vibrations

(29) Bopp, P. *Chem. Phys.* **1986**, *106*, 205.
(30) LaPlaca, S. I.; Hamilton, W. C.; Kamb, B.; Prakash, A. *J. Chem. Phys.* **1973**, *58*, 567.
(31) Bopp, P., unpublished results.
(32) Bopp, P. In *Interactions of Water in Ionic and Nonionic Hydrates*; Kleeberg, H., Ed.; Springer Verlag: Berlin, Heidelberg, New York, 1987; pp 23–26.
(33) Kleeberg, H.; Heinje, G.; Luck, W. A. P. *J. Phys. Chem.* **1986**, *90*, 4427. Lindgren, O.; Kristiansson, O.; Paluszkiewicz, C. In *Interactions of Water in Ionic and Nonionic Hydrates*; Kleeberg, H.; Ed.; Springer Verlag: Berlin, Heidelberg, New York, 1987; pp 43–46.

are virtually identical within the error margins and resemble the spectrum for the parallel motions of the hydration water molecules, in keeping with the interpretation given above (Figure 7). The bands are slightly more asymmetric here and have a maximum at about 290 cm^{-1}. Furthermore, the near identity of the two bands in Figure 10 indicates that there is only very little coupling between the stretching vibrations of two adjacent water molecules.

Acknowledgment. Financial support by the Deutsche Forschungsgemeinschaft is gratefully acknowledged.

Appendix

In order to separate the various librational and vibrational modes of the water molecules, a scheme has been employed which has been used already successfully for the separation of the vibrational modes.[29] The procedure is as follows: The instantaneous velocities of the two hydrogen atoms in the center-of-mass system are projected onto the instantaneous unit vectors (i) in direction of the corresponding O–H bond ($\vec{u}_1$ and $\vec{u}_2$), (ii) perpendicular to the O–H bonds, in the plane of the molecule, pointing outward ($\vec{v}_1$ and $\vec{v}_2$), and (iii) perpendicular to the plane of the molecule ($\vec{p}_1$ and $\vec{p}_2$).

With the use of capital letters to denote the projections of the hydrogen velocities onto the corresponding unit vectors, the following quantities are defined:

$$Q_1 = U_1 + U_2 \qquad R_x = V_1 - V_2$$
$$Q_2 = V_1 + V_2 \qquad R_y = P_1 + P_2$$
$$Q_3 = U_1 - U_2 \qquad R_z = P_1 - P_2$$

where Q_1, Q_2, and Q_3 describe approximately the three normal mode vibrations usually referred to as symmetric stretch, bend, and asymmetric stretch, respectively. R_x, R_y, and R_z approximate the instantaneous rotation around the three principal axes of the water molecule, as defined in the insert of Figure 8. The Fourier transformations of the acfs of these quantities result in the spectral densities of the corresponding modes.

The advantage of the present method resides in the fact that only instantaneous values of geometries and velocities are used. No reference to a hypothetical equilibrium geometry of the molecules has to be made. The quality of the separation achieved has to be judged from the spectral densities obtained.

Registry No. H_2O, 7732-18-5; $SrCl_2$, 10476-85-4.

Electroneutrality Coupling of Electron Hopping between Localized Sites with Electroinactive Counterion Displacement. 1. Potential-Step Plateau Currents

Claude P. Andrieux and J. M. Savéant*

Laboratoire d'Electrochimie Moléculaire de l'Université Paris 7, Unité Associée au CNRS No. 438, 2 place Jussieu, 75251 Paris Cedex 05, France *(Received: December 23, 1987)*

Electroneutrality coupling of electron hopping between localized redox sites and electroinactive counterion displacement induces a "migration" enhancement of the potential-step plateau current responses. This is investigated for systems containing fixed redox ions, mobile electroinactive counterions, and fixed "supporting" electroinactive counterions under semi-infinite diffusion–migration conditions. The current response is easily computed as a function of the ratio of the "mobility" of the electrons and the mobility of the electroinactive counterions and of the relative excess of supporting counterions. The effect of the latter is to suppress the contribution of migration. As the mobility of the electroinactive counterions decreases, the current response increases as a consequence of migration. The dependency of the apparent electron-hopping "diffusion" coefficient upon the concentration of electroactive material goes beyond the simple proportionality reaching eventually a cubic dependence when the mobility of the electroinactive counterions is much lower than the mobility of electrons. This behavior is illustrated with an experimental example taken from literature data. How the ratio between the reduction current of the fully oxidized film to the oxidation current of the same fully reduced film depends upon the various experimental parameters is also discussed.

Introduction

Electron hopping between localized sites, for example, in redox polymers,[1] is necessarily accompanied by the displacement of electron transfer inactive ("electroinactive") counterions so as to maintain electroneutrality. The question thus arises of the effect of the electroinactive counterion displacement on the rate of charge transport in such systems.[2] If electron hopping could be likened with an ordinary ion displacement, as is sometimes done,[3] this would amount to investigating the diffusion and migration of electrons and counterions as coupled by electroneutrality, both obeying the classical Fick and Nernst–Planck laws. This picture is not in fact quite correct since the electron actually hops between two adjacent redox sites of different oxidation states. As shown earlier,[4] as far as charge transport under a concentration gradient is concerned, this is formally equivalent to a "diffusion" (obeying Fick's law) of the two immobile redox sites with the same diffusion coefficient, $D_E = k^\circ_E \Delta x^2 C^\circ_E$ (k°_E, bimolecular electron-transfer rate constant at zero driving force; C°_E, total redox site concentration; Δx, mean distance between two adjacent redox sites). The effect of an electric field is formally equivalent to "migration" of the immobile redox centers with the same mobility. It does not, however, obey the classical Nernst–Planck law but rather a second-order law deriving from the bimolecular character of electron hopping as opposed to the monomolecular character of

(1) For an overview, see: Murray, R. W. In *Electroanalytical Chemistry*; Bard, A. J., Ed.; Dekker, New York, 1984; pp 191–368.

(2) (a) Based on a large body of previous experimental data by various workers, a general discussion of the factors controlling charge transport in redox polymer films is given in ref 1, pp 334–339; see also ref b–l. (b) Facci, J. S.; Schmehl, R. H.; Murray, R. W. *J. Am. Chem. Soc.* **1982**, *104*, 4959. (c) Buttry, D. A.; Anson, F. C. *J. Am. Chem. Soc.* **1983**, *105*, 685. (d) Majda, M.; Faulkner, L. R. *J. Electroanal. Chem.* **1984**, *169*, 77. (e) *Ibid.* **1984**, *169*, 97. (f) Elliott, C.; Redepenning, J. G. *Ibid.* **1984**, *181*, 137. (g) Chen, X.; He, P.; Faulkner, L. P. *Ibid.* **1987**, *222*, 223. (h) Jernigan, J. C.; Murray, R. W. *J. Phys. Chem.* **1987**, *91*, 2030. (i) Jernigan, J. C.; Murray, R. W. *J. Am. Chem. Soc.* **1987**, *109*, 1138. (j) Lange, R.; Doblhofer, K. *J. Electroanal. Chem.* **1987**, *216*, 241. (k) Doblhofer, K.; Lange, R. *J. Electroanal. Chem.* **1987**, *229*, 239. (l) Feldman, B. J.; Murray, R. W. *Inorg. Chem.* **1987**, *26*, 1702.

(3) Buck, R. P. *J. Electroanal. Chem.* **1987**, *219*, 23.

(4) (a) Andrieux, C. P.; Savéant, J. M. *J. Electroanal. Chem.* **1980**, *111*, 377. (b) Laviron, E. *J. Electroanal. Chem.* **1980**, *112*, 1.

0022-3654/88/2092-6761$01.50/0